Evolution of the local structure with hydrogenation in Ti-Zr-Ni quasicrystals and approximants

2002 J. Phys.: Condens. Matter 14 6413

(http://iopscience.iop.org/0953-8984/14/25/310)

INSTITUTE OF PHYSICS PUBLISHING JOURNAL OF PHYSICS: CONDENSED MATTER

J. Phys.: Condens. Matter **14** (2002) 6413–6426 PII: S0953-8984(02)33562-8

Evolution of the local structure with hydrogenation in Ti–Zr–Ni quasicrystals and approximants

A Sadoc[1,2], E H Majzoub[3], V T Huett[4] and K F Kelton[4]

[1] Laboratoire de Physique des Matériaux et des Surfaces, Université de Cergy-Pontoise, Neuville sur Oise, 95031 Cergy-Pontoise Cedex, France
[2] Laboratoire pour l'Utilisation du Rayonnement Electromagnétique, CNRS, MENESR, CEA, Bâtiment 209D, Centre Universitaire Paris-Sud, BP 34, 91898 Orsay Cedex, France
[3] Sandia National Laboratories, 7011 East Avenue, Livermore, CA 95441, USA
[4] Department of Physics, Washington University, St Louis, MO 63130, USA

E-mail: Anne.Sadoc@lpms.u-cergy.fr

Received 7 February 2002, in final form 2 April 2002
Published 14 June 2002
Online at stacks.iop.org/JPhysCM/14/6413

Abstract

The effect of hydrogenation on the local structure of Ti–Zr–Ni alloys has been studied by means of extended x-ray absorption fine structure. The alloys were either icosahedral quasicrystals or crystalline approximants. They were loaded to different hydrogen-to-metal ratios $1.2 \leqslant \mathrm{H/M} \leqslant 1.7$. The desorption process was also investigated by studying the local order in an alloy charged to $\mathrm{H/M} = 1.2$ then desorbed to $\mathrm{H/M} = 0.84$. The local structure was identical in the crystalline and quasicrystalline alloys with the same H/M ratio (0 or 1.2) and that of the desorbed sample was intermediate between that of the non-hydrogenated samples and that of the samples charged to 1.2. Therefore, it is possible to follow the evolution of the local structure with hydrogenation from $\mathrm{H/M} = 0$ to 1.7. A general increase of all the mean first distances was found except for the Zr–Ni (Ni–Zr) one. There is a remarkable inversion of the atomic subshells of titanium and nickel in the first environment of zirconium atoms around $\mathrm{H/M} = 1$. For the 1.56 hydrogenated sample, the effect of adding a small amount of lead, which stabilizes the icosahedral phase, was studied and it was demonstrated that lead atoms substitute for the nickel atoms and are, therefore, incorporated into the quasilattice.

1. Introduction

Titanium/zirconium-based quasicrystals and their related alloys are able to absorb and desorb considerable quantities of hydrogen, making them of potential use for hydrogen storage and battery applications [1, 2]. These alloys are expected to contain a high number of short-range-ordered tetrahedral structural units, which are favourable to occupation by hydrogen. This encourages hydrogen absorption investigations for these alloys.

Recently, we reported extended x-ray absorption fine-structure (EXAFS) measurements of the local order in an icosahedral $Ti_{45}Zr_{38}Ni_{17}$ quasicrystal and in bcc $Ti_{50}Zr_{35}Ni_{15}$, the 1/1 approximant of the icosahedral phase [3]. Alloys hydrogenated to a hydrogen-to-metal ratio (H/M) of 1.7 for the icosahedral phase and 1.4 for the crystalline phase were also studied. Although there is great similarity in local order between the non-hydrogenated quasicrystals and 1/1 approximants, this is not the case after hydrogenation. Whether this is due to an intrinsic difference between the two Ti–Zr–Ni phases, crystalline and quasicrystalline, or to a dependence on the hydrogen concentration could not be determined from these measurements. Moreover, only alloys with a very high H/M ratio were studied and it was rather difficult to interpret the drastic changes observed in the local structures of these very hydrogenated alloys. At the same time, x-ray diffraction only showed a monotonic increase of the lattice parameter, the crystalline or quasicrystalline phase being retained up to the highest H/M ratios. Although the EXAFS technique, like the x-ray diffraction technique, is not directly sensitive to the presence of hydrogen, it allows the study of the average change in local order induced by hydrogen. Therefore, we have undertaken an EXAFS study of the evolution of the short-range ordering as a function of the hydrogen content in Ti–Zr–Ni alloys, crystal or quasicrystal, to complement the information on the averaged, long-ranged ordering available from diffraction measurements, thereby advancing understanding of the hydrogenation. New EXAFS experiments have been performed for smaller H/M ratios, 1.2 and 1.56, above the Ti, Zr and Ni K edges. Moreover, we also attempt to achieve a better understanding of the hydrogenation–dehydrogenation process in these Ti–Zr–Ni alloys from EXAFS experiments performed on an alloy hydrogenated to $H/M = 1.2$, then desorbed to $H/M = 0.84$.

Recently, it was found that small additions of lead increase the stability of the quasicrystalline phase to much higher annealing temperatures [4]. The Pb also causes an expansion of the quasilattice, observed in the x-ray diffraction pattern. In order to determine the location of the lead atoms in the sample, we have performed EXAFS experiments at the L_{III} Pb edge in an icosahedral sample containing Pb (1 at.%) and loaded to $H/M = 1.56$. The local structure around the Pb atoms was compared with the local structures found around the Ti, Zr and Ni atoms in the same sample to determine whether the Pb atoms are located in the grain boundaries or in the quasilattice.

2. Methods

2.1. Experimental details

Samples of the $Ti_{45}Zr_{38}Ni_{17}$ icosahedral-phase quasicrystal and the $Ti_{50}Zr_{35}Ni_{15}$ 1/1 bcc approximant (W phase) were prepared and characterized at the Department of Physics of Washington University (St Louis). Alloy ingots of the desired composition were first produced by arc-melting mixtures of the pure elements on a water-cooled copper hearth in a high-purity argon gas. The icosahedral-phase quasicrystal and the W-phase approximant were obtained following subsequent annealing procedures described elsewhere [2]. The samples were loaded with hydrogen from the gas phase to $H/M = 1.2$ and 1.7 for the icosahedral phase and 1.4 for the W phase [5]. A 1/1 $Ti_{50}Zr_{35}Ni_{13}Pd_2$ sample loaded to $H/M = 1.2$ was also studied. Moreover, an icosahedral $(Ti_{41.5}Zr_{41.5}Ni_{17})_{99}Pb_1$ alloy loaded to $H/M = 1.56$ was investigated in order to determine the location of the lead atoms. The coherence length of this sample was around 400 Å. This is in contrast to the 170 Å coherence length of the other samples. In the following discussion, the samples of the icosahedral and 1/1 alloys will be designated as 'i' and '1/1', respectively, and the hydrogenated ones will be designated as 'i + H/M' and '1/1 + H/M', respectively. Prior to exposure to hydrogen, the samples were first plasma etched in argon

and coated with a thin layer of Pd (about 20 nm) [6]. The Pd coating protects the samples from oxidation on subsequent exposure to air and enhances the dissociation of molecular hydrogen. The phase purity of the samples was confirmed by x-ray diffraction, except for the i + 1.56 sample, where 10% of hydride phase was found. The hydrogenation–dehydrogenation process was studied in an icosahedral $Ti_{45}Zr_{38}Ni_{17}$ alloy hydrogenated to H/M = 1.2, then desorbed to H/M = 0.84. Samples were hydrogenated at 350 °C using a computer-controlled modified Sievert apparatus, described elsewhere [7]. The hydrogen was desorbed by pumping the sample chamber while annealing at 400 °C. The values of H/M were determined from the mass change.

The EXAFS experiments were performed on powdered samples sieved below 50 μm. They were carried out at the Laboratoire pour l'Utilisation du Rayonnement Electromagnétique (LURE, Orsay) using the DCI synchrotron radiation facility on the experimental station EXAFS 13. The x-ray absorption spectra at the Ti, Ni and Zr K edges (4966, 8331 and 17 998 eV respectively) were collected in transmission mode, at low temperature (10 K). The Ti K absorption edge was scanned with a Si(111) double-crystal monochromator detuned by 50% for harmonic rejection; the Ni and Zr edges were scanned using a Si(331) channel-cut single-crystal monochromator. The intensity of the beam before (I_o) and after (I) the sample was measured with the ionization chambers filled either with Ar (Zr edge) or air (Ti and Ni edges). The spectrum at the Pb L_{III} edge (13 055 keV) was recorded in fluorescence mode at ambient temperature. The x-ray wavelength was monitored with a Si(111) channel-cut single-crystal monochromator and the detection was performed by a Canberra multicanal detector (seven elements). I_f is the sum of the fluorescence intensities measured by the seven elements. For reference samples and for energy calibration of the EXAFS apparatus, titanium, nickel, zirconium and lead foils were used.

2.2. EXAFS analysis

Standard procedures of normalization and background removal were followed to determine the EXAFS oscillations, χ, versus the energy, E, of the photoelectron from the absorption coefficient, $\ln I_o/I$ in transmission mode or I_f/I_o in fluorescence mode using a program package [8, 9]. The data were then converted to k-space using $\hbar^2k^2/2m = E - E_0$, where E_0 is the threshold energy origin. The normalized EXAFS signals are very similar for the icosahedral and 1/1 alloys, not only for the non-hydrogenated samples but also for the samples loaded to the same H/M (1.2). This removes the alternative in our previous conclusions [3] and the differences observed in the local order in the 1/1 + 1.4 and i + 1.7 samples appear to be due to a dependence on hydrogen concentration and not to an intrinsic difference between the two Ti–Zr–Ni phases, crystalline and quasicrystalline. Moreover:

- the spectra of the hydrogenated samples (icosahedral or 1/1 phases) are very different from those of the non-hydrogenated ones, even for the less hydrogenated sample (the desorbed sample, H/M = 0.84);
- there is a general tendency for the EXAFS oscillations to shift to lower k-values when H/M increases, according to the simple idea that the interatomic distances increase together with the lattice parameter.

The spectrum obtained at the Pb L_{III} edge is compared in figure 1 to those obtained at the Ti, Zr and Ni K edges for the same i + 1.56 alloy. It is rather difficult to decide, from these raw data, whether lead substitutes for titanium, zirconium or nickel, and whether it is incorporated in the quasilattice or localized only in the grain boundaries.

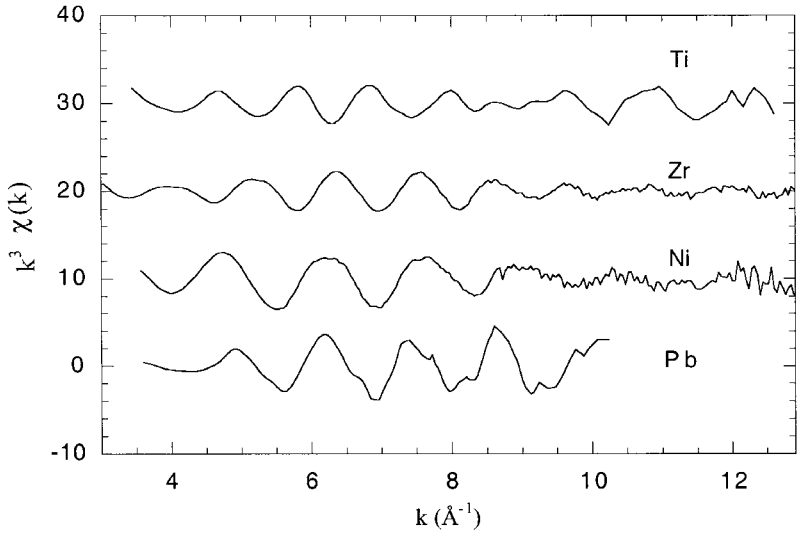

Figure 1. EXAFS spectra above the Ti, Ni, Zr K edges and Pb L_{III} edge in the icosahedral $(Ti_{41.5}Zr_{41.5}Ni_{17})_{99}Pb_1$ alloy loaded to H/M = 1.56.

The Fourier transforms (FTs) of these data for $k^3\chi(k)$ were obtained within a k-window from roughly 3 to 12 Å^{-1} (figures 2, 3 and 4 for respectively the Ti, Zr and Ni edges). The FTs are qualitatively similar to the radial distributions of the atoms neighbouring the absorbing atom (Ti, Ni, Zr or Pb). However, the peaks are shifted to lower R-distances, because of the phase shifts experienced by the photoelectron while scattering from the potentials of the absorbing atom and nearest neighbours. While the FTs look very similar for the i and 1/1 samples, they show drastic differences between the non-hydrogenated alloys and the hydrogenated ones. The FTs are composed primarily of peaks of first neighbours (1.5–4 Å range), but peaks of second neighbours and even further shells clearly appear in the 4–6 Å region in the non-hydrogenated alloys. After hydrogenation, the broad band in the 4–6 Å region, i.e. for intermediate-range order, strongly decreases or even disappears, which may indicate a more disordered structure. Moreover, the FTs obtained for the most hydrogenated sample (i + 1.7) appear significantly different from those obtained for smaller H/M at the Ti edge and also, to a lesser degree, at the Zr edge.

A smaller k-window, up to only 9.6 Å^{-1}, was used for the FT of the Pb L_{III} spectrum due to the smaller extent of this spectrum. Therefore, FTs of the Ti, Ni and Zr spectra were also calculated using this same short k-window to compare directly the pseudo-radial distributions of atoms around each type of atom in the i + 1.56 sample (figure 5). Although the FT at the Pb edge is not identical to any of the other ones, there is some resemblance to that obtained at the Ni edge, but it is shifted to higher R-values at the Pb edge.

To compare the first coordination shell around Ti, Zr, Ni and Pb atoms in the different samples, the first peaks between roughly 2 and 4 Å were backtransformed to k-space. These Fourier-filtered spectra were fitted using the following formula [10], which in single-scattering theories describes the EXAFS oscillations for a Gaussian distribution of neighbours around a central atom:

$$\chi(k) = -\sum_j \frac{N_j}{kR_j^2} B_j(k) \exp\left(-2\sigma_j^2 k^2 - \frac{2R_j}{\lambda}\right) \sin(2kR_j + 2\delta_1' + \phi_j(k)). \quad (1)$$

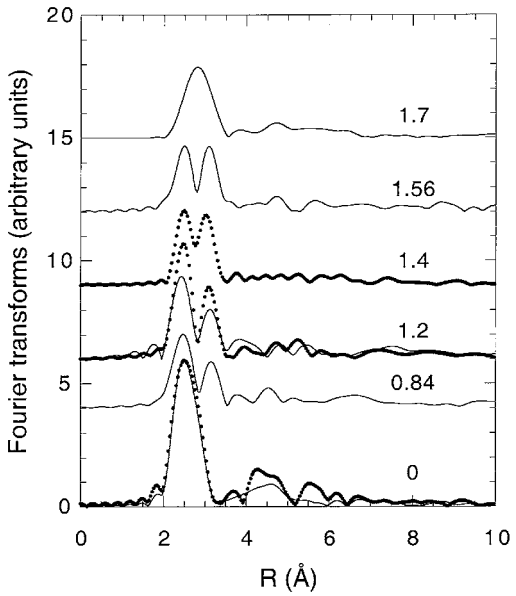

Figure 2. Moduli of the FTs at the Ti K edge in the icosahedral (solid curve) and in the 1/1 (dots) Ti–Zr–Ni alloys studied.

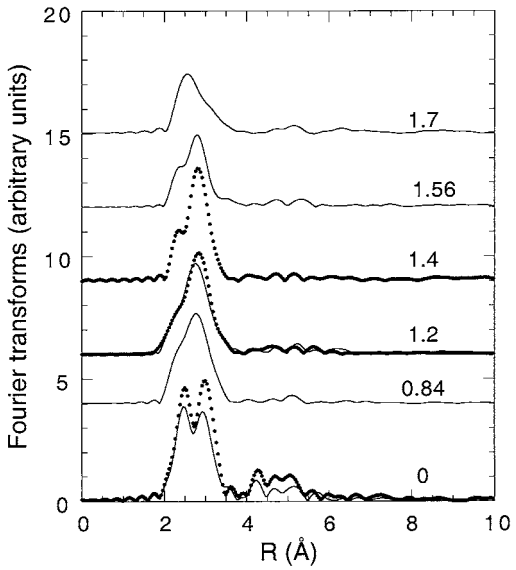

Figure 3. Moduli of the FTs at the Zr K edge in the icosahedral (solid curve) and in the 1/1 (dots) Ti–Zr–Ni alloys studied.

The sum is taken over shells with N_j atoms at distances R_j from the absorbing atom. σ_j is the mean square relative displacement of the absorber and j-backscatter atoms, so the Debye–Waller factor $\exp(-2\sigma_j^2 k^2)$ is a measure of both static and dynamic disorder in shell j. It arises mainly from structural disorder since the experiments were mostly made at low temperature. $B_j(k)$ and $\phi_j(k)$ are the backscattering amplitude and the phase shift respectively,

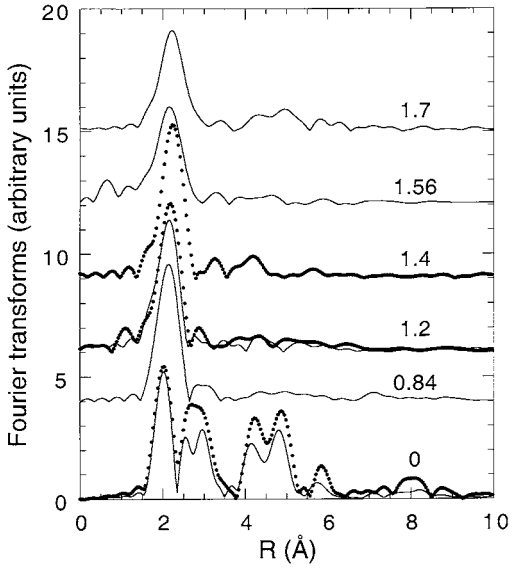

Figure 4. Moduli of the FTs at the Ni K edge in the icosahedral (solid curve) and in the 1/1 (dots) Ti–Zr–Ni alloys studied.

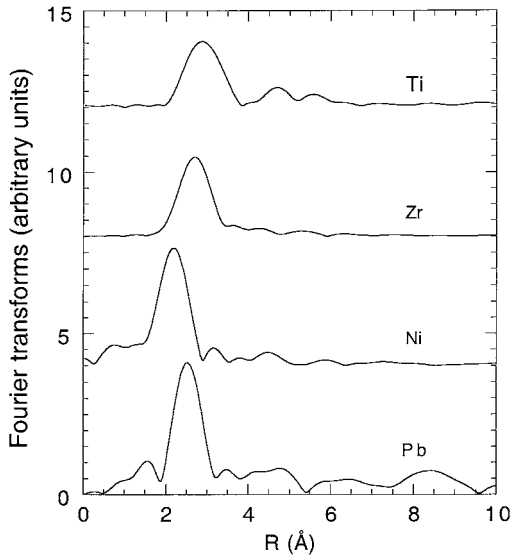

Figure 5. Moduli of the FTs at the Pb L_{III} edge and at the Ti, Zr and Ni K edges in the icosahedral $(Ti_{41.5}Zr_{41.5}Ni_{17})_{99}Pb_1$ alloy loaded to H/M = 1.56.

experienced by the photoelectron while being scattered by the neighbours; δ_1' is the phase shift of the central atom and λ is the electron mean free path. The amplitudes and phase shifts were taken from McKale *et al* [11]. The fitting of the first-neighbour peak in the FT was performed in both *k*- and *R*-space.

A structural model of the W phase [12] was used to analyse the EXAFS spectra of the approximant. Then, the local structure of the non-hydrogenated quasicrystalline phase and of

the hydrogenated alloys was derived from that of the W phase. The number, N, of nearest neighbours was fixed to the values found in the Hennig *et al* model [12] of the 1/1 phase, while the distances, R, and the disorder parameter, σ, were adjusted to fit the calculated spectra to the experimental data. The EXAFS spectra were reconstructed using the distances and disorder parameters of table 1 and typical fits in k- and R-spaces are shown in figure 6 for the Zr edge of the 1/1 phase.

3. 1/1 approximant and icosahedral phase

In the refined structure of the W phase based on x-ray and neutron diffraction measurements [13] and *ab initio* calculations [12], the basic cluster is the Bergman-type cluster, the centre being fully occupied by a nickel atom. The nickel atom is surrounded by 12 titanium atoms making a nearly undistorted icosahedron. A larger, second-shell, icosahedron is filled with 12 titanium/zirconium atoms. The unit cell is represented in figure 7. The numbers and average distances of nearest neighbours are summarized in table 1. All distributions of distances are broad.

Around a titanium atom, there are nickel, titanium and zirconium neighbours which all contribute to the first-neighbour peak in the FT at the Ti edge. Around nickel, there are, on average, 2.8 titanium first neighbours located at a well-defined distance of 2.44 Å and 2.8 titanium atoms at a mean distance of 2.73 Å, plus a few more titanium neighbours at distances beyond 3 Å. The first peak at about 2 Å in the FT of the Ni-edge EXAFS data is due to the shortest Ni–Ti correlation (2.44 Å), while the second one is due to titanium and zirconium neighbour atoms at larger distances from the nickel (2.7–3.24 Å). Around a central zirconium atom, using a cut-off distance of 3.5 Å, there are 8 titanium, 4.5 zirconium and 2.75 nickel neighbour atoms. The contributions of these different types of atom to the imaginary part of the FT are shown in figures 6(c)–(e). When they are out of phase with the imaginary part, their effect is to reduce it and, consequently, the modulus of the FT. Titanium atoms contribute mainly in the 2.5 Å region and zirconium atoms in the 3 Å region. However, the contribution of the nickel atoms is out of phase with the total imaginary part and, therefore, reduces the imaginary part and, also, the modulus of the FT. In fact, the modulus of the FT is not the sum of the moduli of the different contributions. Therefore, the shape of the modulus of the FT does not provide a simple explanation of the environments of the atoms or interpretation of the evolutions of these environments. Simulations have to be done.

In the 1/1 phase, good agreement with the diffraction results was obtained for the average distances determined by means of EXAFS, since the distances differ by <0.10 Å (table 1). There is also a good correlation of the distances and disorder parameters obtained for the heterogeneous pairs from the different edges. It should be kept in mind that the distributions of distances are very broad in the 1/1 phase, which prevents a precise determination of the distances using EXAFS.

For the icosahedral phase, the R-values are very near those found for the 1/1 phase (table 1), which agrees with the similarity observed in the EXAFS spectra and FTs of the icosahedral and 1/1 phases. Therefore, local icosahedral order is found in both types of alloy and the approximants mimic quasicrystals. Somewhat greater σ-values were found, which take into account the reduction of the signals and their FTs in the i phase. This could mean either that the icosahedral phase is more disordered than the 1/1 phase, or that it has a broader distribution of distances.

Table 1. First environments in Ti–Zr–Ni and Ti–Zr–Ni:H icosahedral alloys or 1/1 approximants. The values for the model are taken from [12]. For the EXAFS data, $\Delta R = \pm 0.05$ Å and $\Delta\sigma = \pm 0.04$ Å.

Central	1/1 model			1/1		i		i + 0.84		i + 1.2		1/1 + 1.2		1/1 + 1.4		i + 1.56		i + 1.7	
atom	$\bar{N}$		$\bar{R}$ (Å)	R (Å)	σ (Å)	R (Å)	σ (Å)	R (Å)	σ (Å)	R (Å)	σ (Å)	R (Å)	σ (Å)	R (Å)	σ (Å)	R (Å)	σ (Å)	R (Å)	σ (Å)
Ti	1	Ni	2.44	2.45	0.105	2.46	0.115	2.60	0.18	2.60	0.19	2.49	0.15	2.62	0.12	2.58	0.12	2.58	0.13
	1	Ni	2.73	2.82	0.08	2.80	0.06	2.82	0.06	2.83	0.06	2.82	0.04	2.84	0.06	2.84	0.07	2.71	0.15
	4.9	Ti	2.90	2.85	0.18	2.85	0.19	2.95	0.24	2.99	0.20	2.88	0.21	3.04	0.19	2.93	0.20	2.95	0.14
	5.1	Zr	3.07	3.02	0.12	3.02	0.13	3.21	0.13	3.22	0.12	3.24	0.13	3.27	0.13	3.25	0.125	3.20	0.14
Zr	8	Ti	3.07	3.05	0.12	3.06	0.135	3.20	0.16	3.24	0.16	3.24	0.17	3.28	0.19	3.20	0.19	3.30	0.16
	2.75	Ni	3.19	3.25	0.09	3.28	0.11	3.22	0.20	3.21	0.18	3.23	0.12	3.25	0.10	3.16	0.14	3.11	0.12
	4.5	Zr	3.27	3.33	0.10	3.34	0.11	3.39	0.12	3.42	0.12	3.43	0.13	3.45	0.14	3.39	0.14	3.50	0.12
Ni	2.8	Ti	2.44	2.48	0.08	2.50	0.10	2.54	0.09	2.56	0.10	2.59	0.09	2.58	0.09	2.62	0.11	2.62	0.11
	2.8	Ti	2.73	2.71	0.09	2.72	0.11	2.70	0.15	2.71	0.14	2.73	0.15	2.75	0.11	2.76	0.16	2.74	0.14
	5.6	Zr	3.19	3.18	0.12	3.18	0.13	3.15	0.18	3.21	0.17	3.18	0.17	3.26	0.17	3.26	0.18	3.10	0.21

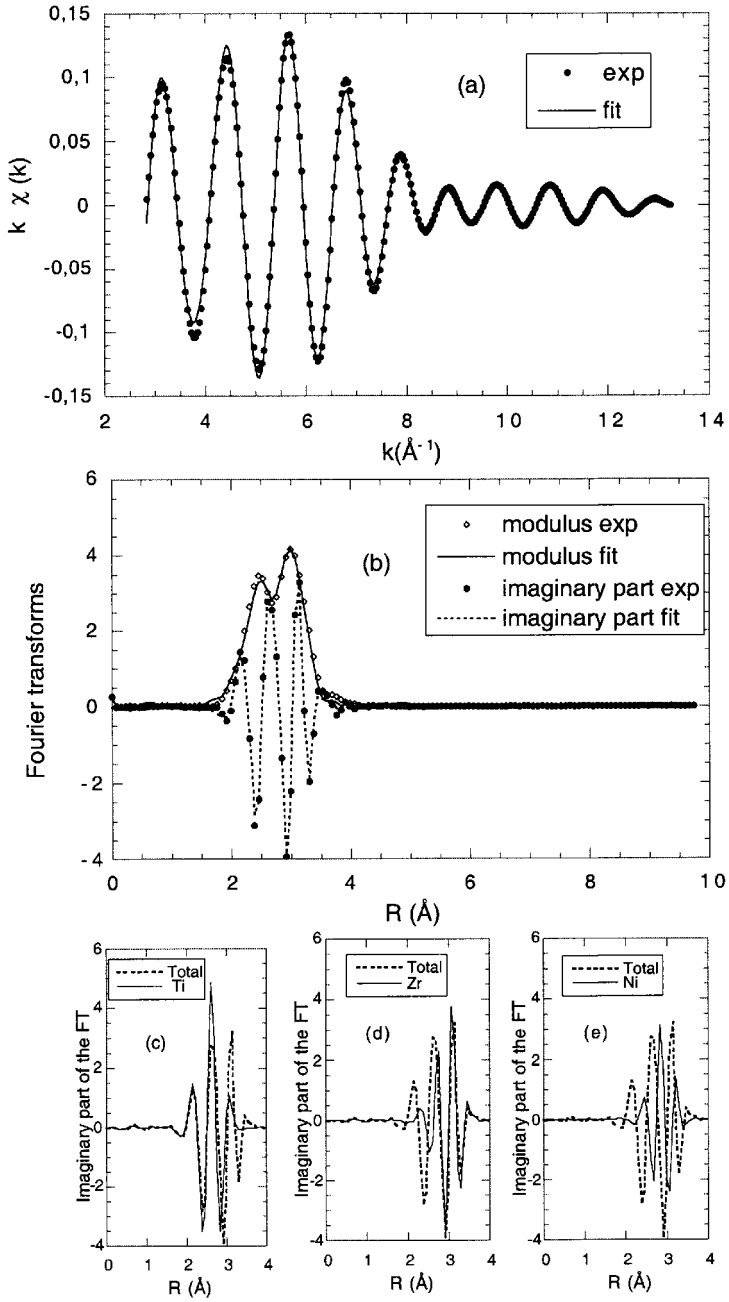

Figure 6. The Fourier-filtered first shell of 1/1 $Ti_{50}Zr_{35}Ni_{15}$ at the Zr edge (a) and the modulus and imaginary part of its FT (b): dots: experiment; curves: calculations. (c), (d) and (e): contributions of the Ti, Zr and Ni neighbour atoms (solid curves) to the imaginary part of the FT (dashed curve).

4. Hydrogenation/dehydrogenation

Assuming that the mean coordination numbers remain unchanged, in particular for the i + 1.56 sample (the composition of which is slightly different from those of the other icosahedral

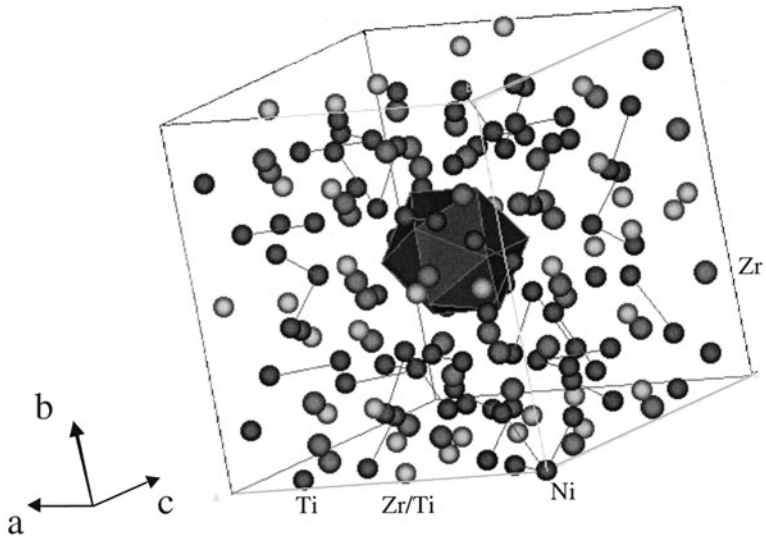

Figure 7. A view of the unit cell of the $Ti_{50}Zr_{35}Ni_{15}$ W phase showing the Ti icosahedron around a central nickel atom.

samples), it was possible to fit all the data correctly. Some previous results, obtained for H/M = 1.7, were reconsidered in order to obtain a somewhat monotonic evolution of the interatomic distances with H/M. The distances and disorder parameters used to fit the spectra are given in table 1. There is a rather good correlation of the distances obtained for the heterogeneous pairs from the different edges. The distances obtained for the sample hydrogenated to H/M = 1.2 then desorbed to 0.84 are intermediate between those for the non-hydrogenated alloy and those for i + 1.2. Therefore, the absorption/desorption process appears to be reversible. Moreover, the desorbed sample could be treated as a sample that was hydrogenated to H/M = 0.84, at least to follow the evolution of the distances with hydrogenation. As for the disorder parameter, the values are very near before (H/M = 1.2) and after desorption.

At the Zr edge, the Zr–Ti and the Zr–Zr correlations contribute respectively to the low-R part and to the high part of the double first-neighbour peak in the FT for H/M = 0. With hydrogenation, the Zr–Ti correlation increases more than the Zr–Zr one. This, together with the increase of the disorder parameter, results in a unique first-neighbour peak in the FT of the hydrogenated alloys. At the same time, the Zr–Ni correlation decreases and its contribution shifts to the low-R side of the first-neighbour peak. At the Ti edge, the Ti–Zr correlation, which is greater than the other correlations, increases more than the other ones. Therefore, the first-neighbour peak, which is unique for H/M = 0, splits into a double peak, the high-R part being due to this Ti–Zr contribution. For H/M = 1.7, the first-neighbour peak is again unresolved due to a smaller value of the Ti–Zr distance. The four correlations all contribute to this unique peak, shifted with respect to that for H/M = 0. The reduction of the modulus of the FT is due, on the one hand, to the fact that the imaginary parts of the different contributions are not in phase and, on the other hand, to an increase of the disorder parameters. At the Ni edge, the peak of first neighbours is split, in the non-hydrogenated alloys, into two components centred at about 2 and 2.75 Å. The Ni–Ti_1 correlation, which corresponds to the narrow peak centred at 2 Å, increases more than the Ni–Ti_2 correlation with hydrogenation. This, together with the decrease of the Ni–Zr distance, results in a unique and broad first-neighbour peak

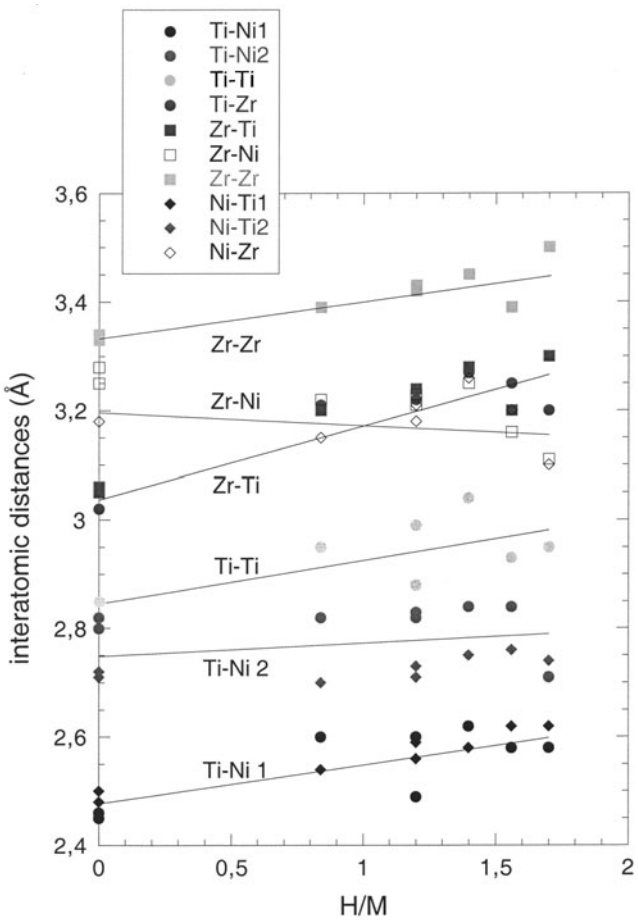

Figure 8. First interatomic distances versus H/M. The lines are guides for the eye.

in the hydrogenated alloys. With hydrogenation, there is a general increase of the disorder parameters, which broadens and reduces the peaks of first neighbours in the FTs. This tendency probably also occurs for a further neighbourhood and is the cause of the strong reduction in the peaks of second-neighbour atoms, or further atoms, observed in the FTs.

The distances are plotted in figure 8 versus H/M for all the correlations. No distinction has been made between the two types of phase, crystalline or quasicrystalline, since very similar fits were obtained for them. The lines are guides for the eye. One can notice that:

- There is a general increase of all the mean distances, except for the Zr–Ni (Ni–Zr) one, in agreement with the increase in the quasilattice constant measured by x-ray diffraction. The increase of the Zr–Ti correlation together with the decrease of the Zr–Ni one result in a remarkable inversion of these distances around $H/M = 1$, which could by no means be conjectured before this study. Consequently, there is an inversion of the titanium and nickel atomic subshells in the environment of Zr atoms. We can, therefore, infer that the introduction of hydrogen in the (quasi)lattice not only induces an expansion of the lattice, but can also bring some atoms closer together.

- The increase is a maximum for the Ti–Zr correlation. Therefore, it can be concluded that the perturbation of the lattice due to hydrogenation is also a maximum around the Ti and Zr atoms and, consequently, that hydrogen atoms sit preferentially near Ti and Zr neighbours, in agreement with previous EXAFS results [3, 14] and nuclear magnetic resonance (NMR) studies [15]. In fact, measurements of the NMR second moment as a function of H/M have been performed on the very same icosahedral $Ti_{45}Zr_{38}Ni_{17}$ quasicrystals. These measurements indicate, in particular, that hydrogen uniformly fills a set of evenly distributed sites in the quasicrystal over $0 < H/M < 1.85$. Calculations of the second moment are consistent with hydrogen preferring sites with a high number of Ti or Zr nearest neighbours.

The changes in the distances are not the same for all types of atom. Therefore, the structure of the hydrogenated alloys is by no means a simple dilatation of that of the non-hydrogenated one. A similar result was obtained recently for $Lu_2Fe_{17}H_x$ ($x = 0, 3$) single crystals, where the Fe–Fe and Fe–Lu interatomic distances do not change equally upon hydrogenation, i.e. the expansion of the crystalline lattice is not isotropic along the different crystallographic directions [16]. The local order in YFe_2D_x ($0 \leqslant x \leqslant 3.5$) deuterides has recently been studied by EXAFS and Mössbauer spectroscopy [17]. Several Fe sites and a large distribution of Fe–Fe distances were observed. These large distance distributions were related to the influence of hydrogen atoms which induce local distortions of the interstitial sites with a displacement of Y and Fe atoms. In Ti–Zr–Ni, the different changes in the distances could also result in large distortions in the local structure. In fact, some larger values of the σ-parameter were indeed generally obtained. Therefore, the hydrogenated alloys appear to be more disordered than the non-hydrogenated ones or have a broader distribution of distances. Another explanation could be that the lattice is less rigid because the bonds are weakened by the presence of H atoms.

The changes in the local structure could affect the physical properties. One could imagine that, if such modifications appear in other metallic compounds, they could contribute to changes observed for example in magnetic properties. In fact, in YFe_2D_x deuterides, the Curie temperature was found to increase for $x = 0$–1.3, then to decrease for $x = 3.5$ [18].

5. Effect of lead atoms

The Pb L_{III} spectrum cannot be simulated using the environments of zirconium or titanium atoms, even with physical changes in R- and σ-values. However, it can be modelled using the environment of nickel atoms with a Pb–Ti_1 distance =2.91 Å, instead of 2.62 Å for the Ni–Ti_1 correlation, and a smaller disorder parameter ($\sigma_{Pb-Ti} = 0.08$ Å instead of $\sigma_{Ni-Ti} = 0.11$ Å). The increase in distance, $\Delta R = 0.3$ Å, takes into account the fact that lead is a bigger atom than nickel (atomic radii: nickel: 1.24 Å; lead: 1.75 Å). The other subshells of atoms are pushed away even more, $\Delta R = 0.8$ Å for the second titanium subshell and 0.5 Å for the zirconium one, with greater disorder parameters (Pb–Ti_2: 3.57 Å; Pb–Zr: 3.76 Å; $\sigma = 0.20$ Å for both pairs). One can conclude that lead atoms substitute for the nickel atoms and that lead appears to be incorporated into the quasilattice, in agreement with the expansion of the quasilattice observed in the x-ray diffraction pattern. The addition of lead increases the stability of the icosahedral phase. Therefore, the fact that the disorder parameter is smaller for the Pb–Ti_1 correlation than for the Ni–Ti_1 one and greater for the two other subshells could imply that the short-range ordering consisting of strong Pb–Ti_1 pairs plays a role in the formation of the icosahedral phase, and the long-range rearrangements of other constitutional elements to form crystalline phases with Ti are restrained. Such an effect was observed in Zr–Al–Ni–Cu metallic glasses, where the addition of Ag and Pd elements is found to be effective for suppressing the grain growth of crystalline phases [19].

6. Conclusions

EXAFS measurements were made in order to elucidate the influence of hydrogen on the structure of the Ti–Zr–Ni alloys, quasicrystals and approximants. Hydrogen concentrations of $H/M = 0$, 0.84, 1.2, 1.4, 1.56 and 1.7 were studied. A first result is that, as for the non-hydrogenated alloys, the local order is very similar in the hydrogenated icosahedral and 1/1 phases. Therefore, the approximants mimic quasicrystals. Secondly, a general increase of all the mean interatomic distances was obtained with increasing hydrogen content, except for the Ni–Zr (Zr–Ni) one, which was found to decrease. The increase of the Zr–Ti correlation together with the decrease of the Zr–Ni one results in a remarkable inversion of the atomic subshells of titanium and nickel around zirconium for a H/M ratio around 1. As the interatomic distances do not change equally upon hydrogenation, the hydrogenation results not only in an expansion of the (quasi)crystal lattice. The increase of distances is a maximum for the Ti–Zr correlation. Therefore, it could be concluded that the perturbation of the lattice due to hydrogenation is also a maximum around Ti and Zr atoms and, consequently, that hydrogen atoms sit preferentially near Ti and Zr neighbours, confirming previous results.

The dehydrogenation process from $H/M = 1.2$ to 0.84 was studied for the icosahedral $Ti_{45}Zr_{38}Ni_{17}$ alloy. The changes in the interatomic distances and, consequently, in the local structure, appear reversible. Finally, the effect of the introduction of a small content of lead atoms, which stabilize the icosahedral phase, was also studied. It was concluded that lead atoms substitute for nickel atoms and that lead appears to be incorporated into the quasilattice.

Acknowledgments

We are pleased to warmly thank our colleagues J Moscovici, A Traverse and F Villain for their help during the EXAFS experiments. K F Kelton gratefully acknowledges the support of the National Science Foundation under grant DMR 00-72787.

References

[1] Viano A M, Stroud R M, Gibbons P C, McDowell A F, Conradi M S and Kelton K F 1995 *Phys. Rev.* B **51** 12 026
[2] Kelton K F, Kim W J and Stroud R M 1997 *Appl. Phys. Lett.* **70** 3230
Kelton K F and Gibbons P C 1997 *MRS Bull.* **22** 69
[3] Sadoc A, Kim J Y and Kelton K F 2001 *Phil. Mag.* A **81** 2911
[4] Davis J P, Majzoub E H, Simmons J M and Kelton K F 2000 *Mater. Sci. Eng.* A **294–6** 104
[5] Kelton K F, Kim J Y, Majzoub E H, Gibbons P C, Viano A M and Stroud R M 1998 *Proc. 6th Int. Conf. on Quasicrystals* ed S Takeuchi and T Fujiwara (Singapore: World Scientific) p 261
[6] Kim J Y, Gibbons P C and Kelton K F 1998 *J. Alloys Compounds* **266** 311
[7] Kim J Y, Majzoub E H, Gibbons P C and Kelton K F 1999 *Mater. Res. Soc. Symp. Proc.* **553** 483
[8] Michalowicz A 1991 EXAFS pour le MAC *Logiciels Pour la Chimie* (Paris: Société Française de Chimie) p 102
[9] Michalowicz A 1997 *J. Physique Coll.* IV **7** C2 235
[10] Stern E A, Sayers D E and Lytle F W 1975 *Phys. Rev.* B **11** 4836
[11] McKale A G, Veal B W, Paulikas A P, Chan S K and Knapp G S 1988 *J. Am. Chem. Soc.* **110** 3763
[12] Hennig R G, Majzoub E H, Carlsson A E, Kelton K F, Henley C L, Misture S, Kresse G and Hafner J 2000 *Proc. 7th Int. Conf. on Quasicrystals; Mater. Sci. Eng.* A **294–5** 361
[13] Kim W J, Gibbons P C, Kelton K F and Yelon W B 1998 *Phys. Rev.* B **58** 2578
[14] Sadoc A, Kim J Y and Kelton K F 1999 *Phil. Mag.* A **79** 2763

[15] Faust K R, Pfitsch D W, Stojanovich N A, McDowell A F, Adolphi N L, Majzoub E H, Kim J Y, Gibbons P C and Kelton K F 2000 *Phys. Rev.* B **62** 11 444
[16] Tereshina I S, Nikitin S A, Stepien-Damm J, Gulay L D, Pankratov N Yu, Salamova A A, Verbetsky V N and Suski W 2001 *J. Alloys Compounds* **329** 31
[17] Paul-Boncour V, Wiesinger G, Reichl Ch, Latroche M, Percheron-Guégan A and Cortes R 2001 *Physica* B **307** 277
[18] Paul-Boncour V and Percheron-Guégan A 1999 *J. Alloys Compounds* **293–5** 237
[19] Saida J, Matsushita M, Li C and Inoue A 2000 *Phil. Mag. Lett.* **80** 737